

# Kinematics of the equine temporomandibular joint

Stephanie J. Bonin, MS; Hilary M. Clayton, BVMS, PhD; Joel L. Lanovaz, MS; Thomas J. Johnson, DVM

**Objective**—To develop a method of measuring 3-dimensional kinematics of the temporomandibular joint (TMJ) in horses chewing sweet feed.

**Animals**—4 mature horses that had good dental health.

**Procedure**—Markers attached to the skin over the skull and mandible were tracked by an optical tracking system. Movements of the mandible relative to the skull were described in terms of 3 rotations and 3 translations. A virtual marker was created on the midline between the rami of the mandibles at the level of the rostral end of the facial crest to facilitate observation of mandibular movements.

**Results**—During the opening stroke, the virtual midline mandibular marker moved ventrally, laterally toward the chewing side, and slightly caudally. During the closing stroke, the marker moved dorsally, medially, and slightly rostrally. During the power stroke, the mandible slid medially and dorsally as the mandibular cheek teeth moved across the occlusal surface of the maxillary cheek teeth. The 4 horses had similar chewing patterns, but the amplitudes varied among horses.

**Conclusions and Clinical Relevance**—The TMJ allows considerable mobility of the mandible relative to the skull during chewing. The method presented in this report can be used to compare the range of motion of the TMJ among horses with TMJ disease or dental irregularities or within an individual horse before and after dental procedures. (*Am J Vet Res* 2006;67:423–428)

Temporomandibular joint motion is affected by dental wear and the presence of malocclusions, but the type and amount of motion at the equine TMJ have not been quantified accurately. Optical motion capture systems are now available that have sufficient accuracy and precision to measure 3-dimensional motion of the TMJ. A prerequisite to evaluating 3-dimensional motion is the establishment of coordinate systems in the segments proximal and distal to the joint. Grood and Suntay<sup>1</sup> developed a system that provides a simple geometric description of the 3-dimensional rotational and translational motion between rigid bodies. Placing markers on key anatomic locations creates segmental joint coordinate systems, such that the axes of the coordinate systems are aligned with anatomic axes of the body segments.

The location of 1 coordinate system relative to another is described either by Euler angles (or Cardan angles) or by the concept of a helical axis. Euler angles are defined as a set of 3 finite rotations assumed to take

place in sequence to achieve the final orientation from a reference orientation.<sup>2</sup> Displacement of a segment from 1 position to another can also be represented as a rotation about and a translation along a particular axis in space called the helical axis or screw axis.<sup>3</sup>

In the study reported here, motion of the mandible relative to the skull will be defined by the following 3 successive rotations: pitch, roll, and yaw,<sup>4</sup> where pitch is a rotation about the transverse horizontal axis, roll is a rotation about the longitudinal axis, and yaw is a rotation about the vertical axis. Fredricson and Drevemo<sup>5</sup> used the same coordinate system to describe equine hoof motion. A complete description of 3-dimensional motion also requires the measurement of translations along 3 axes, which will be described in the rostrocaudal, dorsoventral, and mediolateral directions.

Human patients with TMJ disorders are clearly separated from asymptomatic subjects by significant differences in the range of mandibular movements, including mouth opening, right and left lateral movements, and protrusive movement of the mandible.<sup>6</sup> Analysis of the human masticatory cycle in the frontal and sagittal planes has shown that TMJ abnormalities are associated with significantly slower chewing cycles, in which the jaws are closed more slowly but opened more rapidly.<sup>7</sup> Furthermore, it is usually possible to use these data to determine whether the left or right joint was compromised. In horses, dental floating has been shown to increase TMJ mobility in the rostrocaudal direction but specific dental abnormalities associated with reduced mobility were not identified.<sup>8</sup> Rostrocaudal mobility of the mandible was assessed by use of a ruler to measure the distance between the rostral aspect of the first upper incisor teeth and the rostral aspect of the first lower incisor teeth when the head was held with the mandible parallel to the ground and with the atlanto-occipital joint fully flexed. There does not appear to have been any accurate measurements of the pattern or amount of motion at the equine TMJ during chewing. The objectives of the study reported here were to develop a method of measuring the normal, 3-dimensional motion of the equine TMJ during chewing with 6 degrees of freedom (3 translations and 3 rotations) by use of Euler angles as the rotational position coordinates and to describe the 3-dimensional movements of the mandible in terms of a virtual marker created midway between the left and right rami in 4 horses chewing sweet feed.

## Materials and Methods

**Animals**—A university committee for animal use and care approved this study. Subjects were 4 horses (1 Thoroughbred, 1 Appaloosa, 1 Hanoverian, and 1 Quarter Horse) 5 to 15 years of age that were in good general and dental health and had no dental irregularities or malocclu-

TMJ Temporomandibular joint

Received June 3, 2005.

Accepted September 7, 2005.

From the Mary Anne McPhail Equine Performance Center, Department of Large Animal Clinical Sciences, College of Veterinary Medicine, Michigan State University, East Lansing, MI 48824.

Funded by the McPhail Endowment.

Address correspondence to Dr. Clayton.

sions. Horses ranged in height from 155 to 168 cm at the withers and in body weight from 515 to 608 kg.

**Kinematic data collection**—Marker locations were clipped, and the skin was cleaned with alcohol. Twelve spherical, reflective, tracking markers, 2.54 cm in diameter, were attached to the skin overlying palpable bony landmarks with cyanoacrylate glue (Figure 1). Two tracking markers were placed on the dorsal midline of the face; 1 was located on the forehead at the level of the orbit, and the second was located approximately 10 cm further rostrally. Five tracking markers were placed on each side of the head in the following locations: middle of the facial crest, rostral part of the facial crest, notch where the facial vessels cross the ventral edge of the mandible, and dorsally and ventrally on the caudal edge of the mandibular ramus. In addition, 4 virtual markers were located over the right and left articular tubercles of the skull and the right and left condylar processes of the mandible.

Kinematic data were collected at a sampling rate of 120 Hz by use of 6 strobed, infrared cameras<sup>a</sup> placed in a semicircle around the volume that would be occupied by the horse's head. Data collection volume, which measured approximately 2 × 1 × 1 m, was calibrated by the motion analysis system.<sup>b</sup>

Data collection began with the recording of 2 stationary files. During the first stationary file, the horse stood with its head in the calibrated volume, with the 12 tracking markers in place and 2 temporary markers attached over the articular tubercles. Data were collected for 1 second at 60 Hz while the horse was stationary (not chewing). Temporary markers were removed from the articular tubercles and attached over the condylar processes of the mandible for the second stationary file. Again, the horse stood in the calibrated volume while data were collected for 1 second at 60 Hz. Temporary markers were then removed. Stationary files were used to calculate locations of the articular tubercles and condylar processes from the positions of the tracking markers during postprocessing of data.

During data collection, tracking markers were recorded at 120 Hz as horses chewed sweet feed.<sup>c</sup> The horse was positioned with its head in the calibrated volume and offered the feed. The horse was allowed to eat uninterrupted for at least 2 minutes before commencing data collection. A data set was considered acceptable if the horse did not move its head out of the calibrated volume, did not make any rapid head movements, and was not in the process of ingesting feed. A single trial consisted of a minimum of 4 chewing cycles, and 6 trials/horse were recorded.

**Data analysis**—Markers were tracked automatically. For the data acquisition setup used in this study, errors in linear

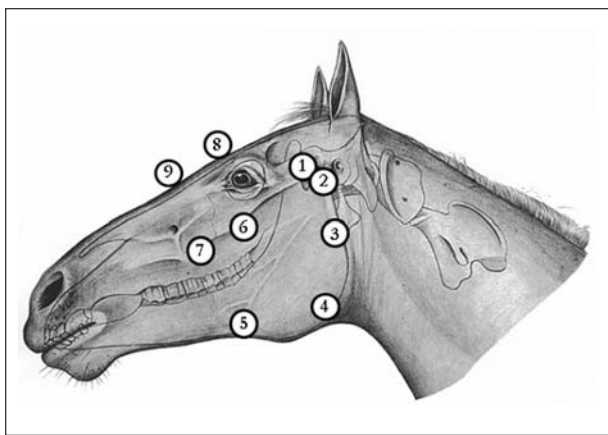


Figure 1—Drawing of temporary marker (1 and 2) locations and tracking marker (3 to 9) locations. Markers 1 to 7 were placed bilaterally; markers 8 and 9 were placed on the dorsal midline.

measurements were < 1 mm.<sup>9</sup> Files were analyzed through a customized program<sup>d</sup> to determine mandibular motion relative to the skull.

Temporary coordinate systems were created on the skull and on the mandible. The origin of the skull coordinate system was located at the forehead marker, and the origin of the mandibular coordinate system was located at the ventral marker on the right ramus of the mandible. These locations were chosen because they appeared to have the least amount of skin displacement relative to the underlying bones during chewing.

Vectors from the local origin to each marker on the segment were determined. A generalized cross-validation was performed on the tracked data to remove high-frequency noise.<sup>3</sup> This technique is a filtering process that fits a cubic spline to the raw data. A transformation matrix and a translation vector were determined by use of a singular value decomposition method on the basis of the work of Soderkvist and Wedin.<sup>10</sup> This algorithm produces a rotation matrix and a translation vector that describe the rotation and translation of the mandibular coordinate system from its neutral position in the standing file to the orientation in each frame of tracked data, while minimizing high-frequency errors that possibly arise from skin displacement. Data were smoothed, and transformations describing mandibular motion were obtained. Orthogonal coordinate systems based on anatomic planes were then established for the skull and mandible. This allowed motions to be described in meaningful anatomic terms. Euler angles were calculated directly as described by Ramakrishnan and Kadaba.<sup>11</sup>

A virtual midline mandibular marker was created and tracked relative to the skull's coordinate system. The purpose of this marker was to aid in viewing mandibular motion and to facilitate comparisons with previous studies<sup>12,e</sup> that estimated relative motion between skull and mandible by tracking markers on the upper and lower lips. The virtual marker was created along the midline of the mandible by use of the mean x-coordinates (rostrocaudal direction) of the rostral facial crest markers and the z-coordinates (dorsoventral direction) of the markers placed over the notch on the mandible from the standing file. The y-coordinate (mediolateral direction) was set equal to zero to place this virtual marker on the midline between the left and right mandibular

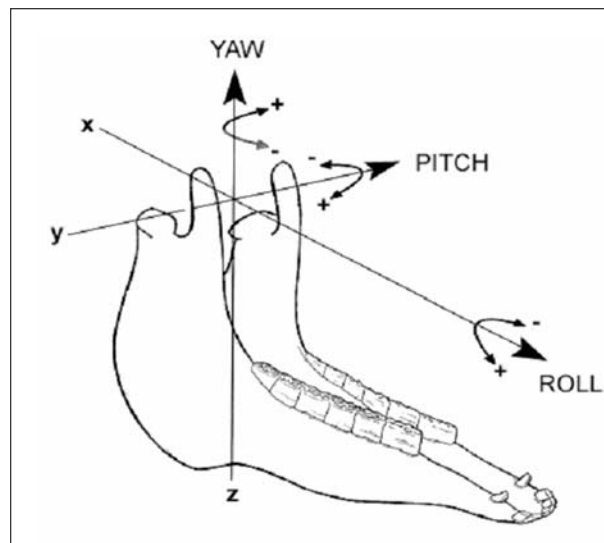


Figure 2—Drawing of axes used to describe mandibular translations and rotations. Notice the positive directions of the x-, y-, and z-axes (straight lines with arrows). Right-handed coordinate systems (curved arrows) are used to define the positive direction of rotations about the x-axis (pitch), the y-axis (roll), and the z-axis (yaw).

rami. This virtual marker was then tracked relative to the skull's coordinate system as a general indicator of mandibular displacement.

All stationary and tracking files were processed with customized software. The output produced 3 Euler angles and 3 translations that described the orientation of the mandible relative to the skull for each frame of data. The coordinate system for the mandible was defined such that the rostrocaudal (x) axis was positive in a rostral direction, the mediolateral (y) axis was positive to the left, and the dorsoventral (z) axis was positive upwards (Figure 2). The 3 translations occur along these axes. Employing the convention of right-handed coordinate systems, positive pitch ( $\alpha$ ) about the y-axis was defined as rotating the mandible to open the mouth and negative pitch was closing the mouth. Positive roll was a counterclockwise rotation ( $\beta$ ) about the x-axis, when viewed from the front of the horse, and negative roll was a clockwise rotation. Positive yaw occurred when the jaw rotated ( $\gamma$ ) counterclockwise about the z-axis, when viewed from above, and negative yaw was clockwise. In addition, the x-, y-, and z-location of the virtual midline mandibular marker relative to the skull's coordinate system was calculated for each frame of data.

Data were processed for the first 3 complete, consecutive chewing cycles in each trial. A cycle was defined from 1 minimum pitch angle to the next, which coincided with the mouth being fully closed. As the mouth opened, the pitch angle increased, and as the mouth closed again, the pitch angle decreased and returned to a minimum value. The chewing side was determined as the side toward which the mandible moved during the closing stroke.

Data were normalized by subtracting the output from the stationary files from the output from the tracking file for all trials. Euler angles and the mandibular translations in each direction were averaged over 60 frames of standing-file data and subtracted from the equivalent values for the tracked files. Likewise, the x-, y-, and z-locations of the virtual midline mandibular marker, averaged over 60 frames of the standing file, were subtracted from values measured in the tracked files. These data are described as normalized.

From the normalized data, the range of angular displacement for pitch, roll, and yaw was calculated as the difference between the maximum and minimum values for each cycle. Translations of the mandible in the rostrocaudal and dorsoventral directions were calculated as the difference between the maximum and minimum values recorded along the x- and z-axis, respectively. Translation in the mediolateral direction was the maximal positive (for horses chewing on the left side)

or maximal negative (for horses chewing on the right side) value of the y-coordinate, expressed as an absolute value. The chewing cycle was divided into 3 phases or strokes. The opening stroke occupied the time between the minimum and maximum pitch angles. It was followed by the closing stroke, which ended when the yaw angle reached its largest absolute value (positive for chewing on the left and negative for chewing on the right). The power stroke, during which the occlusal surface of the mandibular arcade grinds across the occlusal surface of the maxillary arcade, occupied the time between the end of the closing stroke and the start of the next opening stroke.

For the virtual midline mandibular marker, displacements in the x- and z-directions were calculated as the difference between the maximum and minimum coordinate values in each direction. Displacement in the y-direction was the maximal displacement to the left (positive value) or right (negative value), expressed as an absolute value. Distances covered by the mandibular marker during the opening and closing strokes were measured.

**Statistical analysis**—Mean  $\pm$  SD values were calculated for the measured variables within horses and for the entire group. Descriptive statistics were calculated by use of commercial software.<sup>†</sup>

## Results

Of the 4 horses, 2 chewed only on the right side during data collection and 2 chewed only on the left

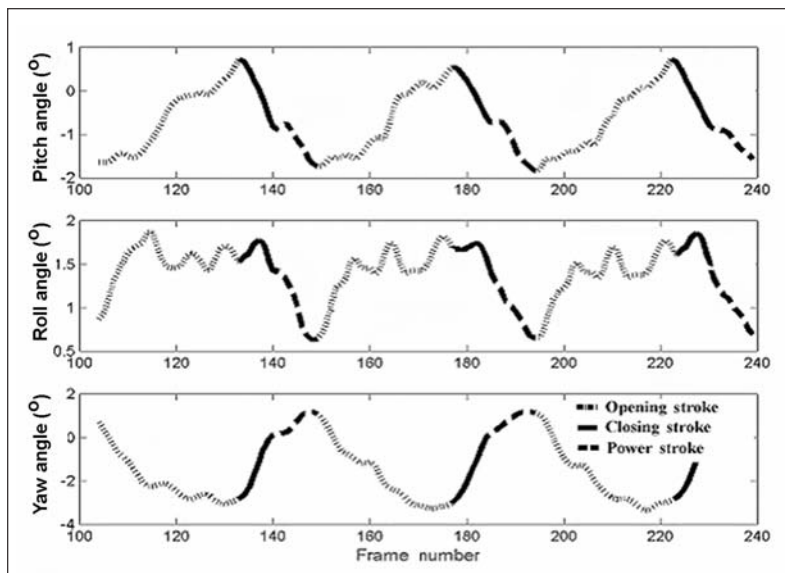


Figure 3—Graphs of Euler angles of pitch (top), roll (middle), and yaw (bottom) versus frame number for 3 successive chewing cycles (1 complete trial) of a horse chewing on the right side.

Table 1—Mean  $\pm$  SD values\* for mandibular rotational and translational ranges of motion in 4 horses.

Variable	Horse 1	Horse 2	Horse 3	Horse 4	Group mean
Ranges of rotational motion					
Pitch (°)	2.25 $\pm$ 0.44	4.58 $\pm$ 0.54	3.45 $\pm$ 0.08	2.58 $\pm$ 0.22	3.22 $\pm$ 0.32
Yaw (°)	2.56 $\pm$ 0.78	3.12 $\pm$ 0.33	3.02 $\pm$ 0.06	3.55 $\pm$ 0.14	3.06 $\pm$ 0.33
Roll (°)	0.55 $\pm$ 0.10	1.05 $\pm$ 0.25	1.26 $\pm$ 0.08	0.72 $\pm$ 0.15	0.90 $\pm$ 0.15
Ranges of translational motion					
Rostrocaudal (cm)	7.58 $\pm$ 0.55	12.87 $\pm$ 2.25	12.30 $\pm$ 0.51	6.65 $\pm$ 0.82	9.85 $\pm$ 1.03
Mediolateral (cm)	2.64 $\pm$ 0.66	10.55 $\pm$ 2.14	4.64 $\pm$ 0.64	7.59 $\pm$ 1.25	6.36 $\pm$ 1.17
Dorsoventral (cm)	2.35 $\pm$ 0.71	4.36 $\pm$ 0.82	4.21 $\pm$ 0.55	2.42 $\pm$ 0.21	3.34 $\pm$ 0.57

\*Values for individual horses are means of 4 trials, each with 3 chewing cycles. Values for group are means of the 4 horses.

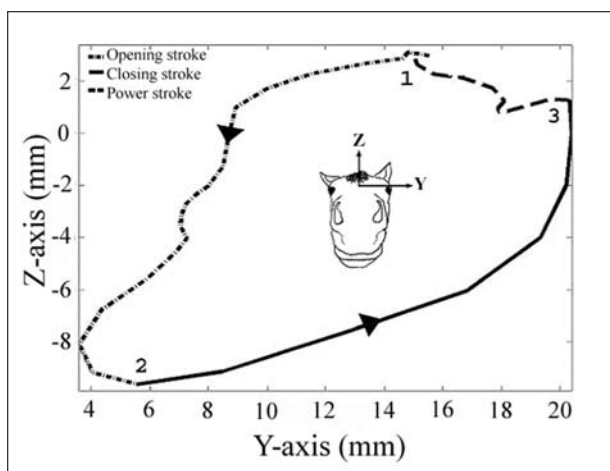


Figure 4—Normalized midline mandibular marker movement in the z-y (transverse) plane from 1 chewing cycle for a horse chewing on the left side. Notice the direction of mandibular motion (arrowheads). 1 = Minimum pitch angle, mandible fully raised, mouth closed. 2 = Maximum pitch angle, mandible fully lowered, mouth open. 3 = Maximum lateral excursion.

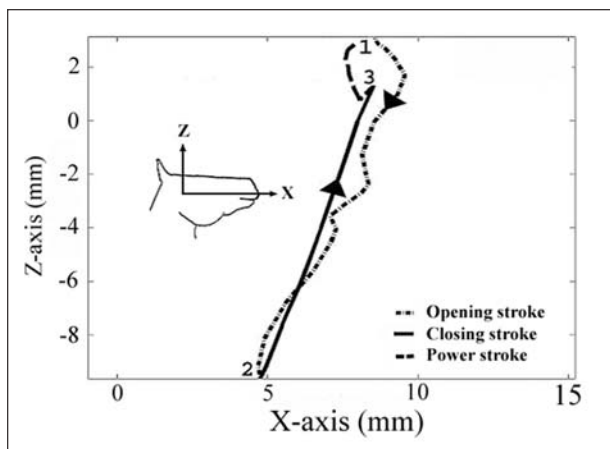


Figure 5—Normalized midline mandibular marker movement in the z-x (sagittal) plane from 1 chewing cycle viewed in the sagittal plane for a horse chewing on the left side. Notice the direction of mandibular motion (arrowheads). See Figure 4 for remainder of key.

side. Three Euler angles were plotted for all trials for a horse chewing on the right (Figure 3). The beginning and end of each cycle were defined from the pitch angles. The beginning of the first cycle was defined by the first minimum pitch angle in the trial, which corresponded with the jaw in its fully closed position. During the opening stroke, the mandible rotated clockwise as seen from the right (positive pitch) until a maximum pitch angle was reached, which corresponded with the fully open position. The direction of mandibular rotation was reversed (negative pitch) during the closing stroke. A change in slope of the pitch angle as the value decreased represented the transition between the closing stroke and the power stroke. When the pitch angle reached a minimum value, the mouth was closed again and the first cycle was complete. Cycles were defined for each trial, and all angles were plotted within the defined ranges. Maximum and minimum angles were averaged for each trial, and the angular dis-

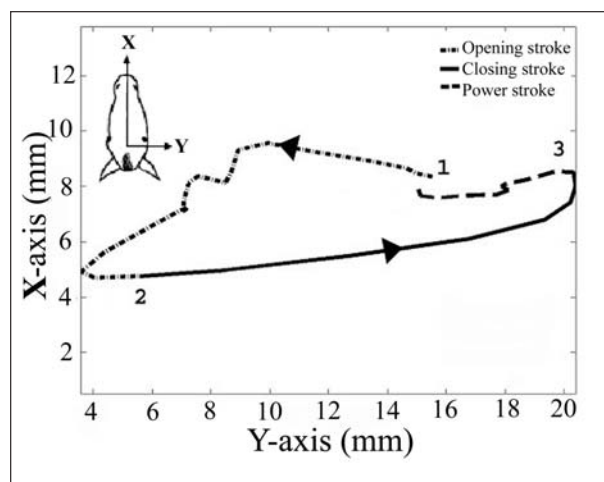


Figure 6—Normalized midline mandibular marker movement in the x-y (dorsal) plane from 1 chewing cycle for a horse chewing on the left side. Notice the direction of mandibular motion (arrowheads). See Figure 4 for remainder of key.

placements were determined for each horse (Table 1). Horses were consistent in the direction of movement, but the amount of motion varied among individuals.

Mandibular kinematics, described in terms of displacement of the virtual midline mandibular marker, were plotted for a horse chewing on the left side in the z-y or transverse plane as seen from in front of the horse's nose, the z-x or sagittal plane as seen from the right of the horse, and the x-y or dorsal plane as seen from above the horse. In the transverse (z-y) plane, the mandible starts in the fully closed position (position 1), then moves ventrally and to the horse's right (negative y), reaching its lowest point (position 2) when the mouth is fully opened. As the mandible is raised, it swings to the horse's left (positive y) to the position of maximum lateral excursion for the cycle (position 3; Figure 4). At this point, the cheek teeth establish contact. The mandible slides to the horse's right and upward to return to the starting position (position 1). The 3 phases of the chewing cycle were easily viewed in this plane as the opening stroke (positions 1 to 2), the closing stroke (positions 2 to 3), and the power stroke (positions 3 to 1).

The sagittal (z-x) plane view of a horse chewing on the left shows that during the opening stroke, the virtual midline mandibular marker moves ventrally (negative z) and slightly caudally (negative x). During the closing stroke, the marker moves rostrally and dorsally, with further dorsal displacement in the power stroke (Figure 5).

In the dorsal (x-y) plane, the mandible moves to the horse's right (negative y) during the opening stroke and slightly caudally (negative x). During the closing stroke, the mandible moves to the horse's left, and then, in the power stroke, it moves to the horse's right (Figure 6). Ranges of motion of the midline mandibular marker in the 3 directions were fairly consistent within and among horses (Table 2). Overall, the midline mandibular marker moved in a caudoventral and lateral direction away from the chewing side during the opening stroke, in a rostradorsal and lateral direction

Table 2—Mean  $\pm$  SD values\* for displacements of midline mandibular marker in 4 horses.

Displacement	Horse 1	Horse 2	Horse 3	Horse 4	Group mean
Rostrocaudal (cm)	3.32 $\pm$ 0.14	5.14 $\pm$ 0.51	4.40 $\pm$ 0.12	5.07 $\pm$ 0.48	4.49 $\pm$ 0.31
Mediolateral (cm)	11.45 $\pm$ 0.25	17.59 $\pm$ 0.69	12.56 $\pm$ 0.40	15.96 $\pm$ 1.74	14.39 $\pm$ 0.77
Dorsoventral (cm)	12.65 $\pm$ 0.18	17.66 $\pm$ 0.67	12.20 $\pm$ 0.28	11.99 $\pm$ 1.24	13.62 $\pm$ 0.60
<i>See Table 1 for key.</i>					

toward the chewing side during the closing stroke, and from a ventrolateral direction to a dorsomedial direction on the chewing side during the power stroke.

## Discussion

An important criterion in selection of a suitable technique for kinematic measurement is that the recording equipment should not alter the characteristics of the movement under study. In human subjects, techniques for measuring TMJ kinematics include attaching magnets to the incisors and tracking their motion with a magnetometer mounted on the skull<sup>13</sup> and using a scintillation detector to track the 3-dimensional motion of a small radioactive source cemented to the skull.<sup>14</sup> Most modern kinematic analysis techniques, however, track the movement of markers attached to the skin overlying anatomically defined landmarks. The amplitude and direction of skin displacement can be expected to vary at different sites, and because the skin displacement is cyclic and has the same frequency as the skeletal cycle, it cannot be detected in raw data.<sup>8</sup> Because skin displacement is a systematic error, it is important to either adhere skin markers to regions with minimal soft tissue motion or to correct for skin displacement. Unfortunately, correction algorithms for skin displacement on the equine head are not available.

In the absence of algorithms correcting for skin displacement in the equine skull and mandible, pilot studies were performed in which markers were placed at sites where skin displacement was expected to be small on the basis of the fact that skin adhered tightly to the underlying bone without the intervention of copious, loose soft tissue. Relative displacements between a large number of marker locations were determined, and locations with the least amount of displacement were chosen for our study.

The transformation matrix obtained through the algorithm of Soderkvist and Wedin<sup>10</sup> more accurately represents the motion of the segment, if the marker set is well configured. Well-configured marker placement requires that the markers have a broad distribution and that they are not placed collinear to each other. If a segment's markers are placed in a straight line and the segment rotates about that line, the motion cannot be detected because the linearly arranged markers do not appear to move to the detection system. Therefore, the more evenly the markers are distributed over the segment, the more accurately the transformation matrix will represent the actual motion. In our study, markers were well distributed over the skull and mandible. A minimum of 3 markers/segment is needed for 3-dimensional tracking, but tracking errors can be reduced by use of a larger number of markers. In our study, 6 markers were used over the mandible and 8 markers were used over the skull.

The masticatory cycle in herbivorous mammals is generally considered to consist of the following 3 events: the opening stroke, the closing stroke, and the power stroke. Collinson<sup>c</sup> described the opening stroke as a downward hinge movement of the mandible mediated by the gliding action of both condyles and the closing stroke as an upward movement combined with a rotation of each condyle in its glenoid cavity. Results of our study indicate that not only is there a downward hinge movement (a pitch rotation about the transverse horizontal axis) during the opening phase, but relatively small rotations also occur simultaneously about the other 2 axes. During the opening phase, the rolling motion seen from the rostral view separates the upper and lower dental arcades on the chewing side. The yaw motion swivels the mandible (crosses the jaw) away from the chewing side. During the closing phase, a small amount of roll assisted in bringing the upper and lower arcades into apposition on the chewing side. The yaw swiveled the mandible toward the midline through the closing and power strokes, which slides the lower arcade across the upper arcade in a lateral to medial direction. The slope of the molar table angle likely dictates the extent of roll angle during the power stroke; a steeper molar table angle will result in more mandibular roll, and a more level molar table will have less mandibular roll.

Previous studies of mandibular motion relative to the skull have been based on tracking movements of the upper and lower lips. Comparisons between the results of our study and those of previous studies<sup>12,c</sup> would have been facilitated by placing a marker along the midline of the mandible. However, the only bony structure on the midline of the mandible is at the mandibular symphysis just caudal to the lower lip. This is not a suitable location for marker placement because the deformability of the soft tissues and the movements of the lips are likely to cause considerable skin displacement artifacts during chewing. To overcome this problem, a virtual marker was created from the locations of the skin markers. The virtual marker was located on the midline between the rami, level with the rostral end of the facial crest and at the height of the mandibular notch. Movements of this marker are easier to view than the mandibular coordinate system translations and rotations, and its movements can be compared with findings in previous studies.<sup>12,15,e</sup>

In previous studies,<sup>12,15,e</sup> the lateral excursion of the equine mandible has been examined. Leue<sup>15</sup> created a mechanical recorder that fit over the rostral portion of the horse's upper and lower jaws and traced the mandibular path while chewing grass, oats, and bran. The mandibular location from which the sketches were created was not indicated. Although Leue<sup>15</sup> did not define the plane that the motion was described in, the

sketches followed the same general pattern as the midline mandibular marker in the x-y (dorsal) plane. Collinson<sup>c</sup> and Baker and Easley<sup>12</sup> measured incisor displacement by marking the upper and lower lips with a continuous line at the junction between the first incisors, recording the mastication sequences from the front of the horse with a video camera, and measuring the displacement from the recording. The lips consist of highly mobile soft tissue and cannot be classified as rigid bodies; therefore, this method of measuring incisor displacement is regarded as approximation only. Although the plane of motion was not identified, the path generated has a similar shape to the midline mandibular marker in the transverse (y-z) plane. In summary, results of our study indicate that 3-dimensional TMJ kinematics can be used to evaluate horses while chewing sweet feed and that mandibular motion follows a consistent pattern within and among horses, with small differences in the amplitude of motion.

- 
- a. Falcon infrared camera, Motion Analysis Corp, Santa Rosa, Calif.
  - b. Motion Analysis Corp, Santa Rosa, Calif.
  - c. Omolene 200, Purina Mills, St Louis, Mo.
  - d. MATLAB, The Mathworks, Natick, Mass.
  - e. Collinson M. *Food processing and digestibility in horses (Equus caballus)*. BSc dissertation, Monash University, Berwick, Australia, 1994.
  - f. SPSS Inc, Chicago, Ill.
  - g. Capozzo A, Gazzani F, Macellari V. Skin marker artifacts in gait analysis (abstr), in *Proceedings*. 6th Meet Eur Soc Biomech 1996;C23.
- 

## References

1. Grood ES, Suntay WJ. A joint coordinate system for the clinical description of three-dimensional motions: application to the knee. *J Biomech Eng* 1983;105:136-144.

2. Kadaba MP, Ramakrishnan HK, Wooten ME. Measurement of lower extremity kinematics during level walking. *J Orthop Res* 1990;8:383-392.
3. Woltring HJ. A FORTRAN package for generalized, cross-validated spline smoothing and differentiation. *Adv Eng Software* 1986;8:104-113.
4. Ostry D, Vatikiotis-Bateson E, Gribble P. An examination of the degrees of freedom of human jaw motion in speech and mastication. *J Speech Lang Hear Res* 1997;40:1341-1351.
5. Fredricson I, Drevemo S. A new method of investigating equine locomotion. *Equine Vet J* 1971;3:137-140.
6. Celic R, Jerolimov V, Knezovic-Zlataric D. Relationship of slightly limited mandibular movements to temporomandibular disorders. *Braz Dent J* 2004;15:151-154.
7. Learreta JA, Bono AE, Maffia G, et al. The identification of temporomandibular joint disease through the masticatory cycle. *Int J Orthod Milwaukee* 2005;16:11-15.
8. Carmalt JL, Townsend HG, Allen AL. Effect of dental floating on the rostrocaudal mobility of the mandible of horses. *J Am Vet Med Assoc* 2003;223:666-669.
9. Lanovaz JL, Khumsap S, Clayton HM, et al. Three-dimensional kinematics of the tarsal joint at the trot. *Equine Vet J Suppl* 2002;34:308-313.
10. Soderkvist I, Wedin P. Determining the movements of the skeleton using well-configured markers. *J Biomech* 1993;26:1473-1477.
11. Ramakrishnan HK, Kadaba MP. On the estimation of joint kinematics during gait. *J Biomech* 1991;24:969-977.
12. Baker G, Easley J. *Equine dentistry*. New York: WB Saunders Co, 2000;30-32.
13. Plesh O, Bishop B, McCall WD. Kinematics of jaw movements during chewing at different frequencies. *J Biomech* 1993;26:243-250.
14. Salomon JA, Waysenson BD. Computer-monitored radionuclide tracking of three-dimensional mandibular movements. Part I: theoretical approach. *J Prosthet Dent* 1979;41:340-344.
15. Leue G, Dobberstein J, Pallaske G, Stunzi H, et al. *Handbuch der Speziellen Pathologischen Anatomie der Haustiere*. 3rd ed. Berlin: Verlag Paul Parey, 1962;131-132.